Materials Chemistry and Physics 132 (2012) 509–514

Contents lists available at SciVerse ScienceDirect

Materials Chemistry and Physics

journal homepage: www.elsevier.com/locate/matchemphys

Morphological effects of reflux condensation on nanocrystalline anatase gel and thin films

Sofia Javed [a,*], Mohammad Mujahid [a], Mohammad Islam [b], Umair Manzoor [c]

[a] School of Chemical and Materials Engineering (SCME), National University of Sciences and Technology (NUST),[1] H-12, Islamabad, Pakistan
[b] Center of Excellence for Research in Engineering Materials (CEREM), College of Engineering, King Saud University,[2] P.O. Box 800, Riyadh 11421, Saudi Arabia
[c] Shaikh Mohammad Alamoudi Chair for Water Researches, Department of Agriculture Engineering, College of Food and Agriculture Sciences, King Saud University,[3] Riyadh, Saudi Arabia

ARTICLE INFO

Article history:
Received 21 March 2011
Received in revised form 21 October 2011
Accepted 24 November 2011

Keywords:
Nanocrystalline titania
Nanostructures
Oxides
Sol–gel growth
Thin films

ABSTRACT

Synthesis of anatase phase of titania is of great interest because of its efficiency in photocatalysis to produce renewable energy in different ways, one being dye sensitized solar cells (DSSC). In the present work reflux condensation is utilized to obtain stable anatase nanostructures from sol gel synthesis using titanium tetraisopropoxide (TTIP) precursor. The refluxing time affects the morphology of as synthesized titania and that of annealed films as well. This variation of morphology is studied and a possible explanation is made. Both XRD and TEM analysis reveal crystallite size to be less than 10 nm. SEM and TEM are used to study morphology which changes from rod like to spherical particles with increasing refluxing time. TGA shows anatase stability upto 700 °C and BET method reveals surface area to be larger than 120 $m^2 g^{-1}$. The films possess great potential for high efficiency when employed in devices.

1. Introduction

Materials with at least one dimension of the order of few nanometers, referred to as nanomaterials or nanostructures, offer great potential in various fields due to their unique electronic, optical, magnetic, chemical, and physical properties [1,2]. Titania (TiO_2) in the form of nanoparticles, nanorods, or thin films has attracted substantial interest due to their unusual optical, electrical and catalytic properties [3]. These unique properties offer their strong potential for application in photocatalysis, photovoltaic devices, and carrier for metallic nanoparticles [4]. Titania minerals naturally occur as three crystallographic phases namely anatase, brookite, and rutile [5]. Anatase is considered to be more important than rutile because it bears better photocatalytic activity due to relatively higher bandgap (3.2 eV) than rutile [6]. There is a great interest in the development of synthetic methods to obtain TiO_2 nanoparticles with phase specificity, well-defined morphology, and high surface area [7]. Generally, it is difficult to produce phase-pure TiO_2 nanoparticles [4] as a mixture of phases has been reported in most cases [5,7,8]. Sol–gel method using titanium alkoxides [4,7,9–16], hydrothermal method [6,17], template-assisted growth [18], anodic oxidation of titanium [19], solvothermal approach [20], or a suitable combination of these are some of the techniques reported for titania synthesis in nanocrystalline form. The morphology and physical/chemical properties of TiO_2 nanostructures depend on particular process, precursor type and concentration, use of capping agents, synthesis temperature, pressure and time [9].

Titania is an important component of dye-sensitized solar cells (DSSCs) whose performance is largely dependent on the optimal properties of the semiconductor layer acting as charge separator. Production of stable nanostructures of anatase with high surface area and porosity is of great interest for researchers to take DSSCs to higher efficiencies with all other advantages. Commercial nanopowder P-25 by Degussa is commonly used for DSSCs but titania prepared by sol gel methods is found to give better performance [21].

In this paper, we present results from low-temperature synthesis of anatase TiO_2 using reflux condensation in sol–gel method. This is the first time that for the synthesis of TiO_2, reflux condensation method was employed in association with sol–gel synthesis as a viable alternative to autoclave treatment. Acetic acid is used to modify the precursor titanium tetra-Isopropoxide (TTIP) to have a controlled sol gel synthesis [22], then, refluxing for different times was carried out to obtain nanostructured TiO_2 with different characteristics. The powders so obtained were used to make paste for subsequent film deposition using doctor blade method. This study

* Corresponding author. Tel.: +92 333 556 1974; fax: +92 51 9085 5002.
E-mail addresses: sofiajaved.nust@gmail.com (S. Javed), mujahids@gmail.com (M. Mujahid), mohammad.islam@gmail.com (M. Islam), umair.manzoor@gmail.com (U. Manzoor).
[1] www.nust.edu.pk
[2] http://cerem-ksu.org/cerem/
[3] www.ksu.edu.sa

0254-0584/$ – see front matter © 2011 Elsevier B.V. All rights reserved.
doi:10.1016/j.matchemphys.2011.11.062

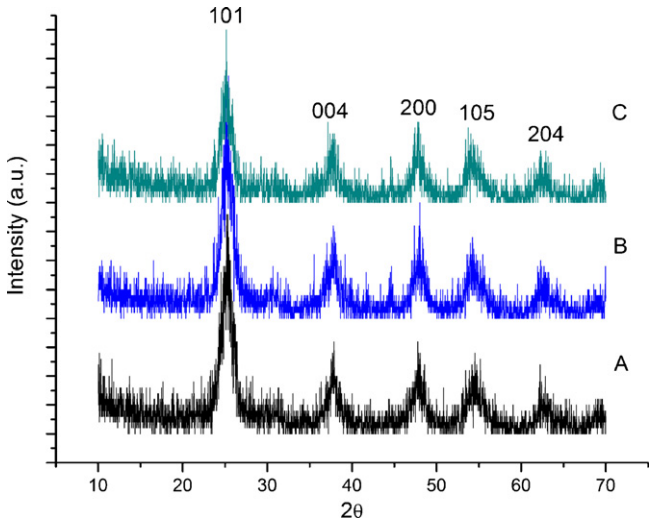

Fig. 1. X-ray diffraction spectra of annealed powders from reflux times of 24 h (A), 70 h (B), and 120 h (C).

resulted in mesoporous TiO_2 films with very high surface area that can be exploited for more efficient charge transfer in DSSCs. The correlation between refluxing and the resulting nanostructures is also explored.

2. Experimental

2.1. Synthesis of titania nanoparticles

All chemicals and materials obtained from Sigma–Aldrich and Merck were of analytical grade and were used without further purification. 12 g (0.2 mol) of glacial acetic acid was added to 56.852 g of Ti (IV) tetraisopropoxide (TTIP) under stirring at room temperature. After 15 min 290 ml of distilled water was added as quickly as possible with vigorous stirring. An instant white precipitate resulted. The mixture was stirred for 1 h to ensure complete hydrolysis. Then 4 ml of concentrated HNO_3 was added and the mixture was heated from room temperature to 80 °C within 40 min and peptized for 75 min. Distilled water was added to make the volume 370 ml. The resulted sol was then subjected to refluxing at 100 °C for different durations i.e. 24 h, 70 h and 120 h.

The gel obtained was exposed to ultrasonics (Cole-Parmer-08895-46 ultrasonic bath) for 20 min. The pH was kept in the range of 1–2. Water was removed form the gel using rotary evaporator and ethanol was added to make 40 wt% TiO_2 gel. The gel was dried at 60 °C and annealed in air at 450 °C for 40 min in Nabertherm Gmbh N17/HR-400V Muffle furnace. The heating rate was kept 1.8 °C per minute.

2.2. Thin films of titania for DSSC

TiO_2 gel, PEG and acetyl acetone (3:3:1), ethanol absolute, and glacial acetic acid were ball milled for 5 days. A few micron thick films over plain glass and transparent conducting oxide (TCO) coated glass were deposited by doctor blading. The films were annealed in a muffle furnace at 450 °C for 40 min at a heating rate of about 1.8 °C per minute.

2.3. Material characterization

The structural and morphological characterization of TiO_2 powders and films was carried out using scanning electron microscope (SEM) (JEOL JSM6460) and transmission electron microscope (TEM) (JEOL 2100). The phase and thermal analysis was done using X-ray diffraction (Stoe D-64295 Darmstadt) and thermogravimetric analysis/Differential thermal analysis (TGA/DTA, Perkin Elmer) techniques. Surface area measurements of TiO_2 films were made using BET method.

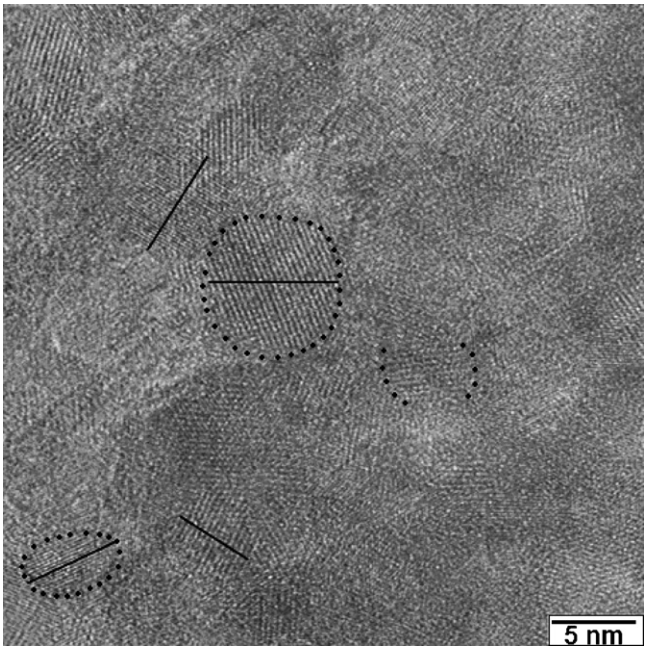

Fig. 2. TEM image of sol gel reflux synthesized anatase with crystallite sizes around 6 nm.

3. Results and discussion

Reflux condensation with sol gel method seems to be an easy low temperature procedure to obtain stable phase pure anatase nanostructures with huge surface area. The method is adopted from Ito et al. [17] till peptization. Afterwards instead of autoclave, reflux condensation is applied and reported for the first time. As we know, sol–gel processes involve metal alkoxides molecules that undergo hydrolysis and subsequently react to condense with each other to form metal–oxygen–metal bridging units. The modification of titanium tetraisopropoxide with acetic acid results in a controlled sol–gel process and it also affects the growth of the

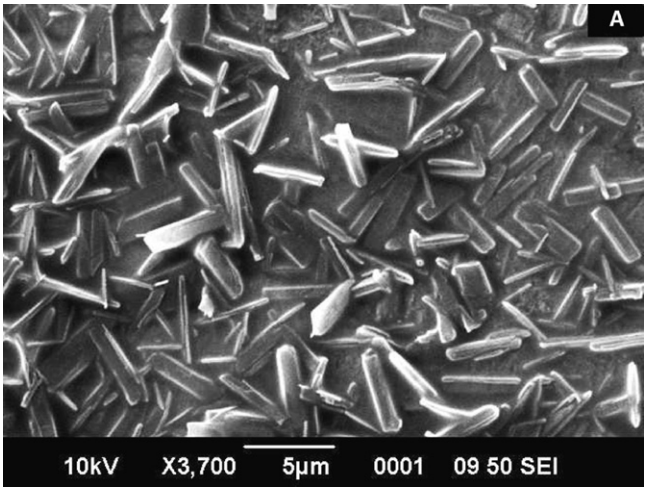

Fig. 3. SEM image of as prepared sample A (24 h refluxed).

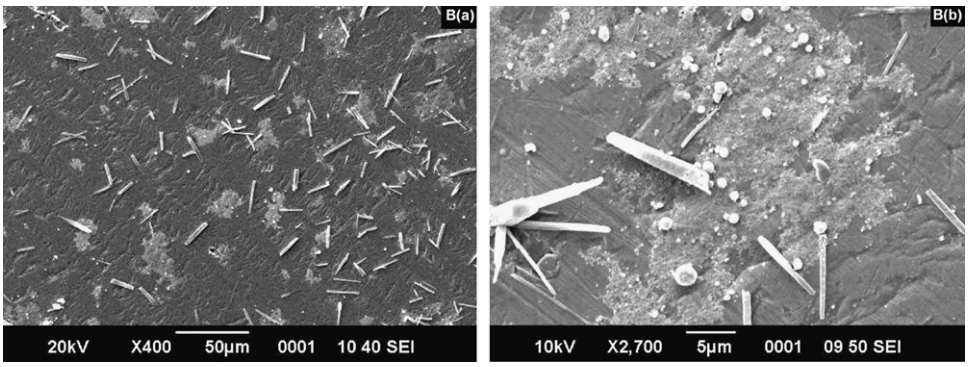

Fig. 4. SEM image of as prepared sample B (70 h refluxed) (a) at 400× (b) at 2700×.

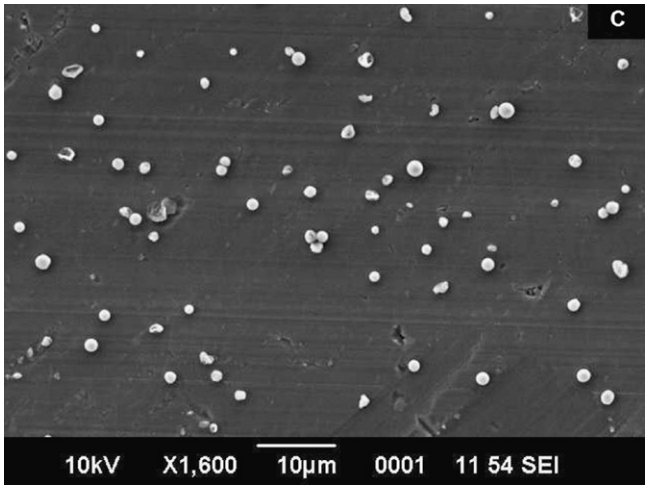

Fig. 5. SEM image of as prepared sample C (120 h refluxed).

resulting product [22,23]. In this work the difference in durations of refluxing at 100 °C has resulted in different morphologies of the obtained product. Both refluxing time and precursor modification have played their role in determining the product morphology. It is speculated that the difference in the thermal energy provided during refluxing for the three kinds of samples has driven the hydrolysis reactions between isopropyl and acetate groups at different rates to give the obtained morphologies. Besides, we have obtained the anatase phase only.

The gel obtained after refluxing at 100 °C consisted of pure anatase titania as revealed by XRD spectra of the samples A (24 h refluxed), B (70 h refluxed) and C (120 h refluxed). XRD after annealing at 450 °C also represents anatase peaks (Fig. 1) i.e. there is no phase change. Due to the inherent nature of sol gel processing route, certain degree of organic residues maybe retained in the powders. It is speculated, however, that the annealing treatment results in burnout of the organic content. Although all major peaks with intensities beyond a certain threshold are indexed to be due to anatase phase, a significant level of background noise in the spectra maybe attributed to the nanocrystalline nature of the powder. From Scherer equation ($t = 0.94\,\lambda/B\cos\theta$, where t is crystallite size, B is the peak width at half maximum and θ being the diffraction angle), the average crystallite size was calculated to be <10 nm for all refluxing times (Table 1).

The findings of crystallite size from XRD data analysis were found to be in agreement with the size of crystallites observed during high-resolution transmission electron microscopy (HR-TEM) examination of the powder particles. A representative TEM micrograph of one of the samples is shown in Fig. 2 where the crystallites in powder particles are revealed using lattice imaging. The crystallites within individual particles can be noticed to be mainly spherical in shape, as indicated by the dotted circles and marked diameters in Fig. 2. The size, as estimated from crystallites seen in the TEM image, is in the range of 5–10 nm. Whereas the size obtained from Scherer equation is based on XRD peak with maximum intensity among all peaks present, HR-TEM micrograph offers a visual examination of the crystallites and supports the results produced from XRD studies.

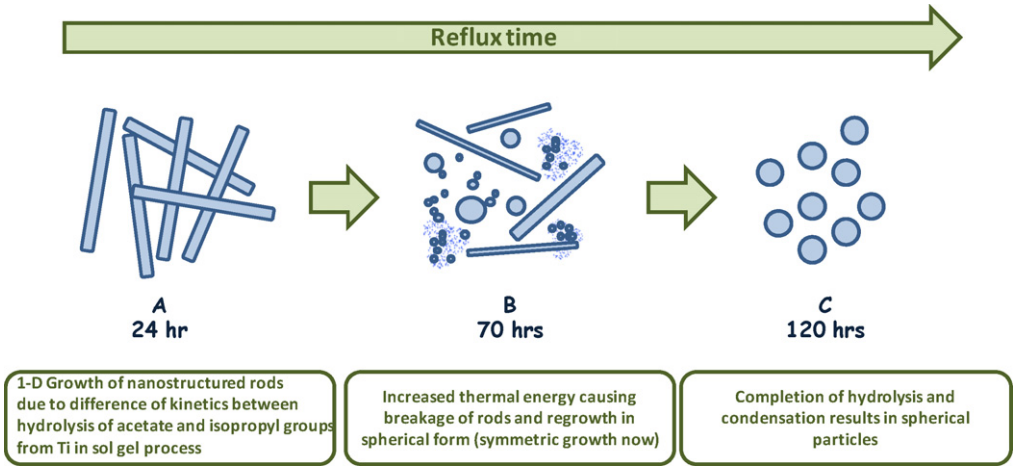

Fig. 6. Schematic for evolution of spherical morphology with increased refluxing time.

Table 1
BET surface area and crystallite sizes (from XRD plots) of samples A–C.

Sr. no.	Reflux time (h)	Sample ID	Crystallite size (nm) before annealing	Crystallite size (nm) after annealing	Surface area ($m^2\ g^{-1}$)
1	24	A	5.4	7.8	160
2	70	B	6.0	9.6	150
3	120	C	5.2	7.3	125

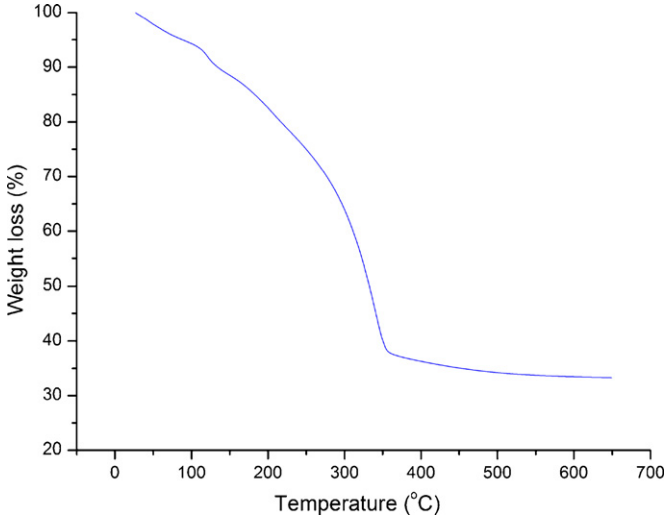

Fig. 7. TG Analysis for (70 h refluxed) sample B.

Refluxing time and acetic acid modification of TTIP has a strong influence on the morphology and distribution of the structures as revealed by SEM micrographs. For 24 h refluxing rod like structures (Fig. 3) are grown which through a mixture of rod like and spherical particles on refluxing for 70 h (Fig. 4a and b) have evolved to spherical particles on 120 h refluxing (Fig. 5).

This can be explained by having an insight into the chemistry of the process. We know that sol gel synthesis involve hydrolysis and condensation of the precursor to form metal oxygen bonds (Ti–O–Ti) in the final product. Acetate modified TTIP gives rise to dimers, trimers or chains of various lengths [22] by condensation between acetate and isopropyl ligands making O bridges between two molecules. It is speculated that for short refluxing times, growth of rod-like structures occurred due to enhanced growth along longitudinal directions due to this reaction. Then during longer refluxing times the other ligands also get hydrolysed and condensed. Rods break due to higher thermal energy provision causing the transition from rod-like to spherical particle morphology (Fig. 6).

Thermal stability of the anatase phase was checked up to 700 °C by testing dried titania pastes in TGA/DTA using air medium. It was observed that there is no phase change up to this temperature. Since all samples exhibited similar behaviour during TGA/DTA studies, the result from only sample B is presented here. The continuous mass loss from room temperature to 400 °C is attributed to the loss of added binder and additional water present as impurity in the material (Fig. 7). The graphical form of the data indicates that at ~550 °C, the net weight loss was approximately 65% which is comparable to the initial loading of TiO_2 in gel. Studies have revealed that PEG pyrolysis and decomposition occurs at temperatures around 400 °C [24,25]. Since TGA/DTA is carried out under air, the decomposition of organic binder is believed to take place at same temperatures during annealing as indicated by TGA. In this regard, the conditions selected for our study are expected to ensure almost complete decomposition of PEG during annealing.

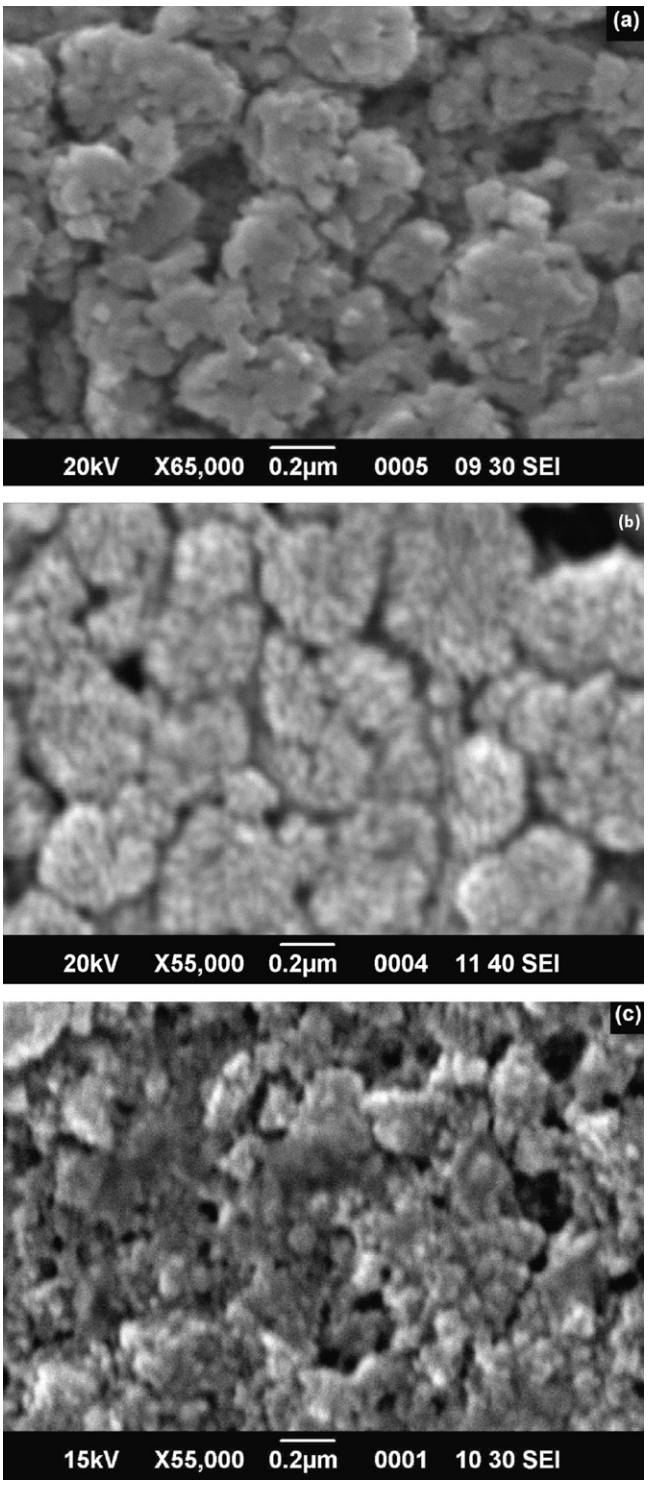

Fig. 8. SEM images of annealed thin films obtained from sol–reflux–gels A (a), B (b) and C (c).

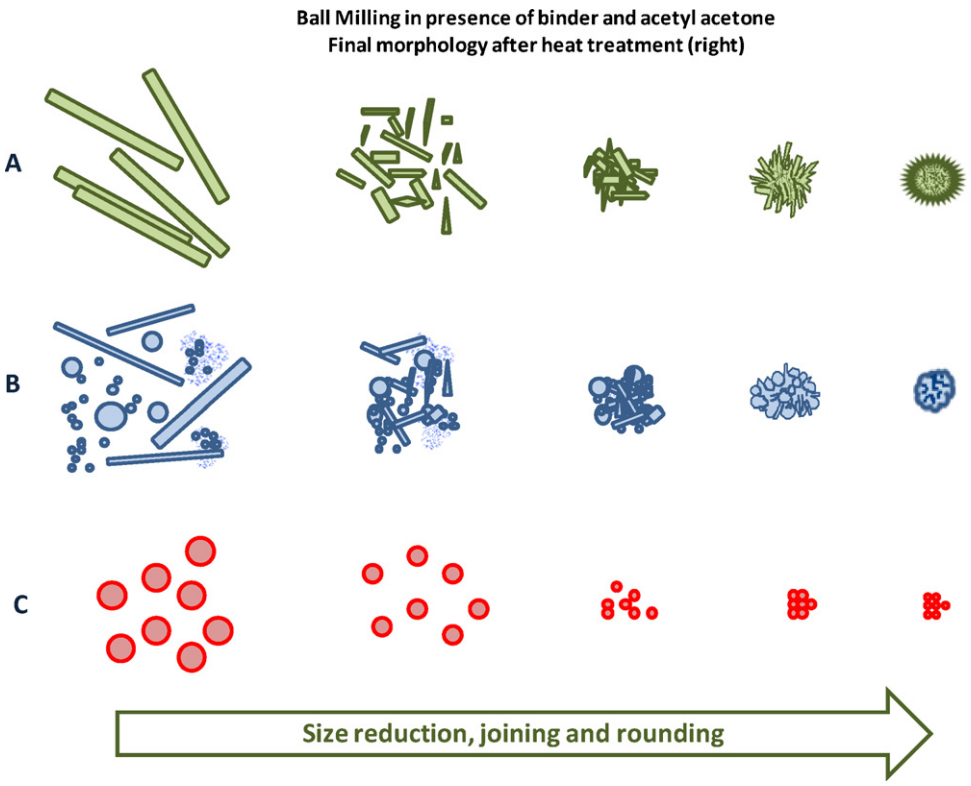

Fig. 9. Schematic for morphology changes in films from as synthesized samples in effect of ball milling.

Thin films produced after 5 days milling of titania gel with binder (PEG) and acetyl acetone were examined topographically using optical microscopy, SEM (before and after annealing) and AFM. The films were annealed at 450 °C, a temperature value chosen on the basis of TGA data that indicated almost no change in mass beyond that (Fig. 7). Although the milling time can be further optimized, a relatively high PEG content with respect to the TiO_2 powder is beneficial, as it not only acts as a binder for improved mechanical stability and pore-forming agent [26], it also improves DSSC performance through formation of a high quality film with flat, even surface and a higher degree of dye adsorption [27].

The surface morphologies of the thin films produced via paste coating are presented in Fig. 8. A schematic representation of the effect of milling and the binder over morphology of the films A–C is given in Fig. 9. These nanostructures obtained after annealing have interesting morphologies which retain the effect of variation in refluxing time. Film A resulted in mesoporous structures consisting of agglomerates with an average size of ~500 nm. As evident in Fig. 8a, these spongy structures are well separated and have pores with typical diameter of the order of <50 nm. From B, nanostructures for whom the reflux time was 70 h, the mixed rod like and spherical particle morphology of nanostructures led to a different film surface microstructure after action of milling and annealing effects. As shown in Fig. 8b, the film reveals nearly round agglomerates, 200 nm in size. Also, these agglomerates can be seen to have smaller secondary particles packed together. The average surface roughness of the film is significantly less with reduced degree of porosity. Similarly the film produced from 'C' gel consists of well distributed nanosized particles with high surface area and good porosity in the film (Fig. 8c) in effect of milling of the relatively larger spherical particles. Annealing resulted in porosity due to removal of organic content. Beside that, the nanoparticles seem to be interconnected to allow proper conduction of the current, when used as photoanode in DSSC.

In general, ball milling resulted in reducing the size of the structures besides acetyl acetone and binder PEG play their roles of surface modification and binding respectively. The annealing has generated nanoporosity in the film structures upon decomposition of the binder PEG.

The surface area values using BET method were obtained for the annealed paste powders, as listed in Table 1. The surface areas can be predicted from Figs. 8 and 9 to be in the order of A > B > C depending upon the morphology of the starting structures and changes brought about by surface modification, size reduction during milling and annealing (binder removal and sintering effects). This is consistent with the values obtained i.e. 160, 150 and 125 $m^2\ g^{-1}$ for films A, B and C respectively. The mesoporosity and high roughness of A films justifies relatively higher value than B films which have a compact structure and poorer porosity. The C films have least value among the three because of the annealing effects which result in compaction of the nanoparticles. This range of surface area values is highly desirable for the use of such powders in DSSC.

4. Conclusion

We have reported a low temperature refluxing process for the production of nanocrystalline phase pure titania with crystallite size of less than 10 nm. The refluxing time and precursor (TTIP) modification (with acetic acid) controls the morphology of the nanostructures and we can obtain rod like or spherical particles or a mixture of both with change in refluxing time. Change in thermal energy and degree of hydrolysis (of acetate groups) during refluxing is considered to bring these structural changes. The structural features of thin films obtained after milling of the nanostructures in presence of acetyl acetone also depict the effect of different refluxing durations. From rod like structures after 24 h refluxing, mesoporous particles of around 500 nm have evolved. And films obtained from nanostructures after 120 h refluxing

consist of spherical particles around 50 nm diameter. So refluxing time has a great influence on the morphology and consequently on other properties like surface area, porosity and roughness of the anatase nanostructures. The thin films obtained for 24 h and 120 h refluxed samples have got nice properties in terms of surface area, morphology and porosity characteristics. These thin films have a potential to be used in photoanodes of DSSCs.

Acknowledgements

We acknowledge National University of Sciences and Technology, Pakistan for providing funds for this work and School of Material Science and Engineering, Nanyang Technological University for providing assistance in performing TEM.

References

[1] E. Serrano, G. Rus, J. Gartia-Martinez, Renew. Sustain. Energy Rev. 13 (2009) 2373–2384.
[2] Y. Azizian-Kalandaragh, A. Khodayari, M. Behboudnia, Mater. Sci. Semicond. Process. 12 (2009) 142–145.
[3] N. Jagtap, M. Bhagwat, P. Awati, V. Ramaswamy, Thermochim. Acta 427 (2005) 37–41.
[4] Y. Ju-Nam, J.R. Lead, Sci. Total Environ. 400 (2008) 396–414.
[5] Y. Li, T.J. White, S.H. Lim, J. Solid State Chem. 177 (2004) 1372–1381.
[6] H. Yin, Y. Wada, T. Kitamura, S. Kambe, S. Murasawa, H. Mori, T. Sakata, S. Yanagida, J. Mater. Chem. 11 (2001) 1694–1703.
[7] J. Yang, H. Peterlik, M. Lomoschitz, U. Schubert, J. Non-Cryst. Solids 356 (2010) 1217–1227.
[8] M. Yan, F. Chen, J. Zhang, M. Anpo, J. Phys. Chem. B 109 (2005) 8673–8678.
[9] M.I. Zaki, A.H. Gamal, Mekhemer, N.E. Fouad, C. Tushar, Jagadale, S.B. Ogale, Mater. Res. Bull. 45 (2010) 1470–1475.
[10] T. Moritz, J. Reiss, K. Diesner, D. Su, A. Chemseddine, J. Phys. Chem. B 101 (1997) 8052–8053.
[11] Z. Zhang, C.C. Wang, R. Zakaria, J.Y. Ying, J. Phys. Chem. B 102 (1998) 10871–10878.
[12] H. Uchida, S. Hirao, T. Torimoto, S. Kuwabata, T. Sakata, H. Mori, H. Yoneyama, Langmuir 11 (1995) 3725–3729.
[13] X. Ding, Z. Qi, Y. He, J. Mater. Sci. Lett. 14 (1995) 21–22.
[14] S. Nishimoto, B. Ohtani, H. Kajiwara, T. Kagiya, J. Chem. Soc.-Faraday Trans. 1 81 (1985) 61–68.
[15] I. Moriguchi, H. Maeda, Y. Teraoka, S. Kagawa, Chem. Mater. 9 (1997) 1050–1057.
[16] C.C. Wang, J.Y. Ying, Chem. Mater. 11 (1999) 3113–3120.
[17] S. Ito, T.N. Murakami, P. Comte, P. Liska, C. Grätzel, M.K. Nazeeruddin, M. Grätzel, Thin Solid Films 516 (2008) 4613–4619.
[18] S.M. Liu, L.M. Gan, L.H. Liu, W.D. Zhang, H.C. Zeng, Chem. Mater. 14 (2002) 1391–1397.
[19] H. Tsuchiya, J.M. Macak, L. Taveira, E. Balaur, A. Ghicov, K. Sirotna, P. Schmuki, Electrochem. Commun. 7 (2005) 576–580.
[20] R.K. Wahi, Y. Liu, J.C. Falkner, V.L. Colvin, J. Colloid Interf. Sci. 302 (2006) 530–536.
[21] C. Longo, M.D. Paoli, J. Braz. Chem. Soc. 14 (2003) 889–901.
[22] P.B. Dunbar, J. Mater. Sci. 35 (2000) 367–374.
[23] K.M.S. Khalil, T. Baird, M.I. Zaki, A.A. E1-Samahy, A.M. Awad, Colloids Surfaces A: Physiochem. Eng. Aspects 132 (1998) 31–44.
[24] K.J. Voorhees, S.F. Baugh, D.N. Stevenson, J. Anal. Appl. Pyrolysis 30 (1994) 47–57.
[25] N. Grassie, G.A. Perdoma Mendoza, Polym. Deg. Stab. 9 (1984) 155–165.
[26] L. Ma, M. Liu, T. Peng, K. Fan, L. Lu, K. Dai, Mater. Chem. Phys. 118 (2009) 477–483.
[27] K. Sakai, Y. Hirashita, T. Aihara, A. Fukuyama, T. Ikari, K. Kukita, S. Furukawa, Thin Solid Films 519 (2011) 5760–5762.